

Effects of Sterics and Electronic Delocalization on the Photophysical, Structural, and Electrochemical Properties of 2,9-Disubstituted 1,10-Phenanthroline Copper(I) Complexes

Mark T. Miller, Peter K. Gantzel, and Timothy B. Karpishin*

Department of Chemistry and Biochemistry, University of California, San Diego,
La Jolla, California 92093-0358

Received January 6, 1999

The syntheses, crystal structures, electronic absorption spectra, electrochemical properties, and photophysical properties of a series of copper(I) bis(phenanthroline) complexes are reported. The phenanthroline ligands that have been prepared and investigated are the following: dop (2,9-di-(2-methylphenyl)-1,10-phenanthroline), xop (2-(2-methylphenyl)-9-(2,6-dimethylphenyl)-1,10-phenanthroline), dpep (2,9-diphenylethynyl-1,10-phenanthroline), and dmesp (2,9-dimesityl-1,10-phenanthroline). The complex $[\text{Cu}(\text{dop})_2](\text{PF}_6) \cdot \text{Et}_2\text{O}$ crystallizes in space group $P\bar{1}$ with $a = 11.854(3) \text{ \AA}$, $b = 14.705(3) \text{ \AA}$, $c = 15.866(4) \text{ \AA}$, $\alpha = 107.81(2)^\circ$, $\beta = 106.72(2)^\circ$, $\gamma = 97.56(2)^\circ$, $V = 2447.6(10) \text{ \AA}^3$, and $Z = 2$. For 5739 unique data with $F > 4.0\sigma(F)$, $R = 7.52\%$. The complex $[\text{Cu}(\text{xop})_2](\text{PF}_6) \cdot \frac{3}{2}\text{CH}_3\text{OH}$ crystallizes in space group $C2/c$ with $a = 23.096(6) \text{ \AA}$, $b = 23.387(6) \text{ \AA}$, $c = 17.873(7) \text{ \AA}$, $\beta = 100.08(3)^\circ$, $V = 9505(5) \text{ \AA}^3$, and $Z = 8$. For 5631 unique data with $F > 4.0\sigma(F)$, $R = 6.02\%$. The complex $[\text{Cu}(\text{dpep})_2](\text{PF}_6)$ crystallizes in space group $P\bar{1}$ with $a = 13.327(7) \text{ \AA}$, $b = 14.114(7) \text{ \AA}$, $c = 15.175(5) \text{ \AA}$, $\alpha = 87.23(4)^\circ$, $\beta = 66.48(3)^\circ$, $\gamma = 61.84(4)^\circ$, $V = 2273(2) \text{ \AA}^3$, and $Z = 2$. For 4851 unique data with $F > 4.0\sigma(F)$, $R = 5.47\%$. The complex $[\text{Cu}(\text{dmesp})(\text{dpep})](\text{PF}_6)$ crystallizes in space group $Pbca$ with $a = 14.547(6) \text{ \AA}$, $b = 22.868(6) \text{ \AA}$, $c = 30.659(10) \text{ \AA}$, $V = 10199(6) \text{ \AA}^3$, and $Z = 8$. For 2281 unique data with $F > 4.0\sigma(F)$, $R = 9.43\%$. The electrochemical, spectral, and structural properties of $[\text{Cu}(\text{dop})_2]^+$ and $[\text{Cu}(\text{xop})_2]^+$ demonstrate that the copper coordination environment is more sterically encumbered and more rigid in these two complexes than the coordination environment in the comparison molecule $[\text{Cu}(\text{dpp})_2]^+$ (dpp = 2,9-diphenyl-1,10-phenanthroline). A larger energy gap is predicted for $[\text{Cu}(\text{dop})_2]^+$ and $[\text{Cu}(\text{xop})_2]^+$ based on these data, and consequently, a blue-shifted emission is observed relative to $[\text{Cu}(\text{dpp})_2]^+$. The room-temperature excited-state lifetimes in dichloromethane and methanol of the dop and xop complexes are shown to be shorter than the dpp complex, and these results are interpreted as due to a reduction in ligand π -electron delocalization in the former two complexes. The complexes $[\text{Cu}(\text{dpep})_2]^+$ and $[\text{Cu}(\text{dmesp})(\text{dpep})]^+$ are shown to have increased ligand π -electron delocalization relative to $[\text{Cu}(\text{dpp})_2]^+$; however, neither complex displays room-temperature steady-state emission in dichloromethane.

Introduction

Photoluminescent inorganic complexes are potentially useful for molecular solar-energy conversion and for molecular sensing. In order for these complexes to be practically useful, strong absorption in the visible region and long ($> 100 \text{ ns}$) excited-state lifetimes in solution are necessary. The majority of work in this area has been on luminescent tris(diimine) complexes of ruthenium and osmium. Although much less studied, certain copper(I) bis(diimine) complexes also absorb strongly in the visible region and display excited-state lifetimes that are sufficiently long for bimolecular quenching.^{1–4} From a practical standpoint, solar-energy conversion devices and sensors based on inexpensive copper are more attractive than systems based on ruthenium or osmium.

Copper(I) forms pseudotetrahedral complexes with diimine ligands such as phenanthroline and bipyridine, and with certain diimine ligands forms complexes that are emissive at room temperature in solution. The most well-studied photoluminescent $[\text{Cu}(\text{NN})_2]^+$ (NN = a 1,10-phenanthroline derivative) complexes

are $[\text{Cu}(\text{dmp})_2]^+$ and $[\text{Cu}(\text{dpp})_2]^+$ (dmp = 2,9-dimethyl-1,10-phenanthroline; dpp = 2,9-diphenyl-1,10-phenanthroline). Work by Blaskie and McMillin initially demonstrated that $[\text{Cu}(\text{dmp})_2]^+$ is emissive in dichloromethane upon excitation into the metal-to-ligand charge-transfer (MLCT) band.⁵ This emission was shown, however, to be quenched in donating solvents such as methanol. It was subsequently shown by the McMillin and Sauvage groups that in methanol, the more sterically encumbered $[\text{Cu}(\text{dpp})_2]^+$ complex remains emissive.⁶ McMillin and co-workers have provided convincing evidence that in the excited state of $[\text{Cu}(\text{dmp})_2]^+$, a donating solvent can act as a Lewis base and form a five-coordinate adduct (exciplex) that decays very rapidly.¹ Although there is no spectroscopic proof for such exciplexes, exciplex quenching is consistent with the tendency for the Cu^{II} complex, $[\text{Cu}(\text{dmp})_2]^{2+}$, to be five-coordinate.⁷ This interpretation would then imply that the phenyl groups in $[\text{Cu}(\text{dpp})_2]^+$ sterically prevent formation of a five-coordinate structure, resulting in emission in donating solvents. Recently, the copper(II) complex $[\text{Cu}(\text{dpp})_2]^{2+}$ was shown to

(1) McMillin, D. R.; Kirchoff, J. R.; Goodwin, K. V. *Coord. Chem. Rev.* **1985**, *64*, 83–92.

(2) Kutal, C. *Coord. Chem. Rev.* **1990**, *99*, 213–252.

(3) Horváth, O. *Coord. Chem. Rev.* **1994**, *135/136*, 303–324.

(4) Ruthkosky, M.; Kelly, C. A.; Castellano, F. N.; Meyer, G. J. *Coord. Chem. Rev.* **1998**, *171*, 309–322.

(5) Blaskie, M. W.; McMillin, D. R. *Inorg. Chem.* **1980**, *19*, 3519–3522.

(6) Dietrich-Buchecker, C. O.; Marnot, P. A.; Sauvage, J.-P.; Kirchoff, J. R.; McMillin, D. R. *J. Chem. Soc., Chem. Commun.* **1983**, 513–515.

(7) van Meerssche, M.; Germain, G.; Declercq, J. P.; Wilputte-Steinert, L. *Cryst. Struct. Commun.* **1981**, *10*, 47–52.

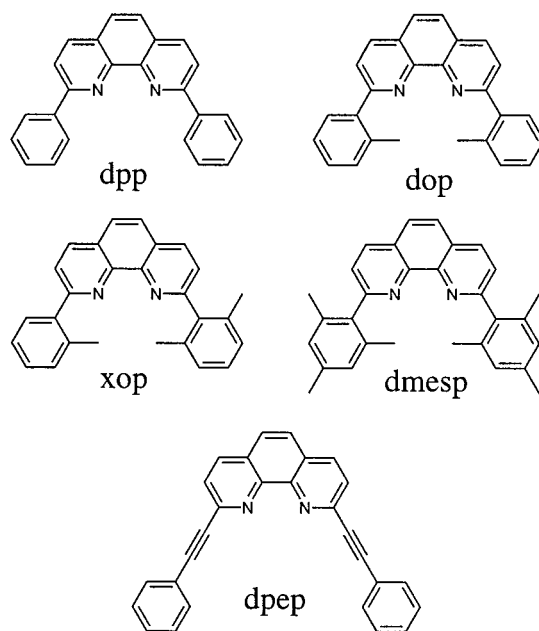
be four-coordinate in donating solvents and in the solid state,⁸ lending support to the notion that $[\text{Cu}(\text{dpp})_2]^+$ remains four-coordinate in the MLCT excited state in all solvents.

Although the coordination number of $[\text{Cu}(\text{dpp})_2]^+$ and $[\text{Cu}(\text{dpp})_2]^{2+}$ is four for both complexes in the solid state, the geometries about the metal ions are significantly different.⁸ Whereas the copper(I) complex displays a distorted tetrahedral geometry, the copper(II) complex is flattened toward a square-planar geometry. In addition, solution-state and solid-state absorption spectra indicate that the geometries in solution and in the solid are similar for both complexes. Since the MLCT excited states of copper(I) complexes exhibit behavior consistent with copper(II) ions,¹ it follows that the ground-state structure of $[\text{Cu}(\text{dpp})_2]^{2+}$ provides a reasonable view of the MLCT excited state of $[\text{Cu}(\text{dpp})_2]^+$. Thus, it can be concluded that, relative to the ground state, a significant "flattening" distortion occurs about the copper ion in the MLCT excited state of $[\text{Cu}(\text{dpp})_2]^+$.

Until recently, the room-temperature excited-state lifetime of $[\text{Cu}(\text{dpp})_2]^+$ was one of the longest for any of the copper(I) bis(phenanthroline) complexes that had been investigated. Eggleston et al. recently reported that the complex of 2,9-di-*sec*-butyl-1,10-phenanthroline, dsbp, has a lifetime that is considerably longer than $[\text{Cu}(\text{dpp})_2]^+$ in dichloromethane: $[\text{Cu}(\text{dsbp})_2]^+$, $\tau = 400$ ns;⁹ $[\text{Cu}(\text{dpp})_2]^+$, $\tau = 250$ ns.^{10–12} The bulky *sec*-butyl groups are believed to reduce the distortion that occurs in the MLCT excited state of $[\text{Cu}(\text{dsbp})_2]^+$ by clashing with the *sec*-butyl groups on the other ligand. Since the interligand interactions prevent the excited state from relaxing toward a flattened square-planar geometry, the $[\text{Cu}(\text{dsbp})_2]^+$ complex emits at higher energy than complexes with smaller substituents at the 2 and 9 positions. The larger energy gap between the ground and emitting state in $[\text{Cu}(\text{dsbp})_2]^+$ is then the likely reason for the longer excited-state lifetime of the complex.¹³

The research described herein focuses on examining the steric and electronic effects that contribute to the excited-state lifetimes of copper(I) bis(phenanthroline) complexes. Recent work has shown that increasing π -delocalization in the ligand can substantially increase the excited-state lifetimes of ruthenium and osmium diimine complexes.^{14–19} Electronic delocalization over an extended π^* orbital reduces the degree of structural distortion in the ³MLCT excited state and results in a smaller equilibrium displacement (ΔQ_e). Decreasing ΔQ_e (the difference between the ground-state and excited-state equilibrium geometries) reduces the amount of vibrational overlap between

Chart 1



the ground and excited states leading to smaller nonradiative decay rate constants (k_{nr}) and longer excited-state lifetimes.¹⁶ Since delocalization in the phenyl groups of dpp is possibly a significant influence on the photophysics of $[\text{Cu}(\text{dpp})_2]^+$, we synthesized the ligand dop and the asymmetric ligand xop (Chart 1). The methyl groups on the *o*-tolyl and xylyl substituents in dop and xop sterically prevent coplanar orientations of the aryl groups with the phenanthroline moiety (*intra*ligand interactions) and thus should decrease the degree of electronic delocalization into the 2 and 9 aryl groups. Investigation of the photophysical properties of the copper(I) complexes of dpp, dop, and xop is then expected to reveal whether the phenyl groups play an electronic as well as steric role in the lifetime of $[\text{Cu}(\text{dpp})_2]^+$. In examining molecular models, however, it is clear that *inter*ligand interactions in $[\text{Cu}(\text{dop})_2]^+$ and $[\text{Cu}(\text{xop})_2]^+$ should also greatly reduce the ability for the copper ion to distort toward a square-planar geometry in the excited state. Thus, a priori, contradictory predictions are plausible in predicting the lifetimes of $[\text{Cu}(\text{dop})_2]^+$ and $[\text{Cu}(\text{xop})_2]^+$ relative to $[\text{Cu}(\text{dpp})_2]^+$. Ligand electronic delocalization arguments would predict shorter lifetimes for the dop and xop complexes, whereas interligand steric arguments would predict a larger energy gap and longer lifetimes relative to the dpp complex.

This paper reports the photophysical properties, solid-state and solution-state structures, absorption spectroscopy, and electrochemistry of the two complexes $[\text{Cu}(\text{dop})_2]^+$ and $[\text{Cu}(\text{xop})_2]^+$, and relates the data to $[\text{Cu}(\text{dpp})_2]^+$. As will be shown, electronic delocalization involving the phenyl groups in complexes with 2,9-diaryl substituents appears to play a central role in the observed excited-state lifetimes. Two additional complexes in which ligand electronic delocalization is increased have also been prepared: $[\text{Cu}(\text{dpep})_2]^+$ and $[\text{Cu}(\text{dmesp})(\text{dpep})]^+$ (Chart 1). The photophysical properties, structures, spectroscopy, and electrochemistry of these complexes have also been investigated. The mixed complex $[\text{Cu}(\text{dmesp})(\text{dpep})]^+$ was prepared in order to increase ligand electronic delocalization while also increasing the rigidity about the copper ion by virtue of the mesityl groups of the dmesp ligand. Although copper(I) complexes are labile in solution, it is demonstrated that mixed phenanthroline complexes such as $[\text{Cu}(\text{dmesp})(\text{dpep})]^+$ can be prepared cleanly.²⁰ In addition,

- (8) Miller, M. T.; Gantzel, P. K.; Karpishin, T. B. *Inorg. Chem.* **1998**, *37*, 2285–2290.
- (9) Eggleston, M. K.; McMillin, D. R.; Koenig, K. S.; Pallenberg, A. J. *Inorg. Chem.* **1997**, *36*, 172–176.
- (10) Ichinaga, A. K.; Kirchoff, J. R.; McMillin, D. R.; Dietrich-Buchecker, C. O.; Marnot, P. A.; Sauvage, J.-P. *Inorg. Chem.* **1987**, *26*, 4290–4292.
- (11) Gushurst, A. K. I.; McMillin, D. R.; Dietrich-Buchecker, C. O.; Sauvage, J.-P. *Inorg. Chem.* **1989**, *28*, 4070–4072.
- (12) Ruthkosky, M.; Castellano, F. N.; Meyer, G. J. *Inorg. Chem.* **1996**, *35*, 6406–6412.
- (13) Meyer, T. J. *Pure Appl. Chem.* **1986**, *58*, 1193–1206.
- (14) Boyde, S.; Strouse, G. F.; Jones, W. E., Jr.; Meyer, T. J. *J. Am. Chem. Soc.* **1990**, *112*, 7395–7396.
- (15) Benniston, A. C.; Grosshenny, V.; Harriman, A.; Ziessel, R. *Angew. Chem., Int. Ed. Engl.* **1994**, *33*, 1884–1885.
- (16) Strouse, G. F.; Schoonover, J. R.; Duesing, R.; Boyde, S.; Jones, W. E., Jr.; Meyer, T. J. *Inorg. Chem.* **1995**, *34*, 473–487.
- (17) Treadway, J. A.; Loeb, B.; Lopez, R.; Anderson, P. A.; Keene, F. R.; Meyer, T. J. *Inorg. Chem.* **1996**, *35*, 2242–2246.
- (18) Grosshenny, V.; Harriman, A.; Romero, F. M.; Ziessel, R. *J. Phys. Chem.* **1996**, *100*, 17472–17484.
- (19) Damrauer, N. H.; Boussie, T. R.; Devenney, M.; McCusker, J. K. *J. Am. Chem. Soc.* **1997**, *119*, 9, 8253–8268.

$[\text{Cu}(\text{dmesp})(\text{dpep})]^+$ is, to the best of our knowledge, the first structurally characterized heteroleptic copper(I) bis(phenanthroline) complex.

Experimental Section

General. All chemicals used were reagent grade and used as received unless otherwise specified. Tetrahydrofuran, diethyl ether, and toluene were freshly distilled from sodium/benzophenone. Dichloromethane and acetonitrile for photophysical and electrochemical studies were Burdick and Jackson high-purity grade and stored over 4 Å molecular sieves under N_2 . The methanol used for photophysical studies was Fisher optima grade and stored over 4 Å molecular sieves under N_2 . Nitrogen used in the syntheses was purified by passing the gas through anhydrous CaSO_4 , 4 Å molecular sieves, and an oxygen scrubbing catalyst ("Ridox", Fisher Scientific). Proton NMR spectroscopy was performed on a General Electric QE300 (300 MHz) Spectrometer or a Varian 400 MHz Spectrometer. Infrared spectra were collected on a Nicolet 510 IR Spectrometer. Electronic absorption spectra were recorded on a Hewlett-Packard 8452A Diode Array Spectrophotometer. Extinction coefficients ($\pm 5\%$) were determined using X-ray quality crystalline material that was thoroughly dried in vacuo. FAB mass spectra were obtained from the Scripps Research Institute mass spectrometry facility. Column chromatography was performed on silica gel 60 from EM Science.

Syntheses. The compounds $[\text{Cu}(\text{CH}_3\text{CN})_4](\text{PF}_6)_2$,²¹ 2,9-diphenyl-1,10-phenanthroline (dpp),²² and 2,9-dichloro-1,10-phenanthroline²³ were synthesized as previously reported. The ligand dmesp was a gift from Craig Woods, prepared using the literature procedure.²⁴

2-(2-Methylphenyl)-1,10-phenanthroline and 2,9-Di(2-methylphenyl)-1,10-phenanthroline (dop). A 1.6 M solution of *n*-butyllithium in cyclohexane (11.0 mL, 17.6 mmol) was slowly added to a solution of *o*-bromotoluene (2.00 mL, 16.6 mmol) in 15 mL of diethyl ether at 0 °C. The solution was allowed to stir for 30 min at 0 °C. This organolithium solution was cannula transferred to an addition funnel which was placed over a suspension of 1,10-phenanthroline (0.720 g, 4.00 mmol) in 10 mL of diethyl ether. The 1,10-phenanthroline solution was cooled to 0 °C, and the organolithium solution was slowly added. The solution became bright red and was allowed to stir overnight at room temperature. The reaction mixture was cooled to 0 °C, and 20 mL of water was added. The layers were separated, and the water layer was extracted three times with 15 mL portions of dichloromethane. The ether and dichloromethane fractions were mixed and stirred with 20 g of activated MnO_2 for 3 h. The mixture was dried with MgSO_4 and filtered, and the filtrate was evaporated to dryness. The resulting solid was separated by column chromatography (SiO_2 , 1:1:1 dichloromethane:ethyl acetate:hexanes). The third of four fractions contained the amber oily disubstituted product, dop (0.048 g, 0.13 mmol, 3.3% yield). ^1H NMR (CDCl_3) δ : 3.64 (s, 6H), 7.33 (m, 8H), 7.63 (d, 2H), 7.80 (d, 2H), 7.83 (s, 2H), 8.30 (d, 2H). FAB-MS m/z (relative intensity): 361 (100) ($\text{M} + \text{H}^+$). The fourth fraction contained the pale yellow monosubstituted product. ^1H NMR (CDCl_3) δ : 2.43 (s, 3H), 7.31 (m, 3H), 7.55–7.65 (m, 2H), 7.74 (d, 1H), 7.75–7.87 (m, 2H), 8.20–8.35 (m, 2H), 9.22 (dd, 1H). FAB-MS m/z (rel intensity): 271 (100) ($\text{M} + \text{H}^+$).

2-(2-Methylphenyl)-9-(2,6-dimethylphenyl)-1,10-phenanthroline (xop). A 1.6 M solution of *n*-butyllithium in cyclohexane (11.0 mL, 17.6 mmol) was slowly added to a solution of 2-bromoxylene (0.250 mL, 1.88 mmol) in 3 mL of diethyl ether at 0 °C. The solution was allowed to stir for 30 min at 0 °C. This organolithium solution was cannula transferred to an addition funnel which was placed over a suspension of 2-(2-methylphenyl)-1,10-phenanthroline (0.250 g, 0.922 mmol) in 5 mL of diethyl ether. The suspension was cooled to 0 °C,

and the organolithium solution was slowly added. The solution became bright red and was allowed to stir overnight at room temperature. The reaction mixture was cooled to 0 °C, and 20 mL of water was added. The layers were separated, and the water layer was extracted three times with 15 mL portions of dichloromethane. The ether and dichloromethane fractions were mixed and stirred with 9 g of activated MnO_2 for 3 h. The mixture was dried with MgSO_4 and filtered, and the filtrate was evaporated to dryness. The resulting solid was separated by column chromatography (SiO_2 , 1:1:1 dichloromethane:ethyl acetate:hexanes). The third of three fractions contained the pale yellow product (0.190 g, 0.507 mmol, 55.0% yield). ^1H NMR (CDCl_3) δ : 2.20 (s, 6H), 2.58 (s, 3H), 7.10–7.33 (m, 6H), 7.55–7.64 (m, 2H), 7.80 (d, 1H), 7.86 (s, 2H), 8.30 (d, 1H), 8.32 (d, 1H).

2,9-Diphenylethynyl-1,10-phenanthroline (dpep). This ligand was synthesized in a manner similar to a published procedure.²⁵ 2,9-Dichloro-1,10-phenanthroline (0.250 g, 1.00 mmol), phenylacetylene (0.237 mL, 2.16 mmol), cuprous iodide (0.008 g, 0.04 mmol), bis-(triphenylphosphine)palladium(II) chloride (0.012 g, 0.017 mmol), triethylamine (0.348 mL, 2.50 mmol), and *N,N*-dimethylformamide (1 mL) were placed in a resealable heavy-walled glass tube containing a Teflon-coated stirbar. The tube was evacuated and flushed with nitrogen several times, capped, and heated with stirring to 90 °C in an oil bath for 24 h. The red reaction mixture was allowed to cool and then poured into 15 mL of water. The water layer was washed four times with 15-mL portions of dichloromethane. The combined dichloromethane washes were evaporated to dryness, and the crude product was purified by column chromatography (SiO_2 , dichloromethane). The second of three bands contained the desired product (0.268 g, 0.704 mmol, 70.4% yield). ^1H NMR (CDCl_3) δ : 7.396 (t, 6H), 7.742 (q, 4H), 7.799 (s, 2H), 7.856 (d, 2H), 8.241 (d, 2H).

General Procedure for $[\text{Cu}(\text{dpp})_2](\text{PF}_6)_2$, $[\text{Cu}(\text{dop})_2](\text{PF}_6)_2$, $[\text{Cu}(\text{xop})_2](\text{PF}_6)_2$, and $[\text{Cu}(\text{dpep})_2](\text{PF}_6)_2$. This procedure is based on previously published procedures.^{8,12} Two equivalents of ligand were dissolved in a nitrogen-saturated solution of 25% dichloromethane in acetonitrile (~10 mL). The acetonitrile solution was slowly added to 1 equiv of $[\text{Cu}(\text{CH}_3\text{CN})_4](\text{PF}_6)_2$ under nitrogen. The solution immediately turned dark red, and the mixture was stirred for 30 min at room temperature. The solution was evaporated to dryness, and the resulting red solid was recrystallized with diethyl ether from dichloromethane. X-ray quality crystals of $[\text{Cu}(\text{dop})_2](\text{PF}_6)_2$ were grown by slow diffusion of diethyl ether into a dichloromethane solution of the complex. X-ray quality crystals of $[\text{Cu}(\text{xop})_2](\text{PF}_6)_2$ and $[\text{Cu}(\text{dpep})_2](\text{PF}_6)_2$ were grown by slowly cooling a refluxing solution of the complex in methanol.

$[\text{Cu}(\text{dpp})_2](\text{PF}_6)_2$. UV-vis: λ_{max} (nm) (ϵ ($\text{M}^{-1} \text{cm}^{-1}$)) CH_2Cl_2 , 440 (3800). ^1H NMR ($\text{DMSO}-d_6$) δ : 6.52 (t, 8H), 6.78 (t, 4H), 7.43 (d, 8H), 8.05 (d, 4H), 8.20 (s, 2H), 8.74 (d, 4H).

$[\text{Cu}(\text{dop})_2](\text{PF}_6)_2$. UV-vis: λ_{max} (nm) (ϵ ($\text{M}^{-1} \text{cm}^{-1}$)) CH_2Cl_2 , 472 (4700). ^1H NMR ($\text{DMSO}-d_6$) δ : 1.79 (s, 12H), 5.91 (t, 4H), 6.70 (t, 4H), 6.83 (d, 8H), 7.95 (d, 4H), 8.75 (d, 4H).

$[\text{Cu}(\text{xop})_2](\text{PF}_6)_2$. UV-vis: λ_{max} (nm) (ϵ ($\text{M}^{-1} \text{cm}^{-1}$)) CH_2Cl_2 , 452 (3.0×10^3). ^1H NMR ($\text{DMSO}-d_6$) δ : 0.80 (s, 6H), 1.39 (s, 6H), 1.99 (s, 6H), 5.93 (d, 2H), 6.36 (t, 2H), 6.45–6.58 (m, 4H), 6.92–7.04 (m, 4H), 7.71–7.84 (m, 4H), 7.89 (d, 2H), 8.23–8.37 (m, 4H), 8.61 (d, 2H), 8.85 (d, 2H).

$[\text{Cu}(\text{dpep})_2](\text{PF}_6)_2$. UV-vis: λ_{max} (nm) (ϵ ($\text{M}^{-1} \text{cm}^{-1}$)) CH_2Cl_2 , 474 (4900). ^1H NMR ($\text{DMSO}-d_6$) δ : 6.49 (d, 8H), 6.98 (t, 8H), 7.25 (t, 4H), 8.20 (s, 4H), 8.21 (d, 4H), 8.79 (d, 4H).

$[\text{Cu}(\text{dmesp})(\text{dpep})](\text{PF}_6)_2$. The mixed ligand complex was prepared by dissolving 1 equiv of dmesp in nitrogen-saturated dichloromethane. One equivalent of $[\text{Cu}(\text{CH}_3\text{CN})_4](\text{PF}_6)_2$ was added to this solution, and the resulting yellow solution was allowed to stir for 10 min at room temperature. The solution turned red upon the addition of 1 equiv of the dpep ligand. This red solution was allowed to stir for 10 min at room temperature. The solution was then evaporated to dryness, and the complex was purified by column chromatography (SiO_2 , ethyl acetate) followed by recrystallization from methanol. The yield of the desired complex was essentially quantitative. UV-vis: λ_{max} (nm) (ϵ ($\text{M}^{-1} \text{cm}^{-1}$)) CH_2Cl_2 , 500 (5300). ^1H NMR ($\text{DMSO}-d_6$) δ : 1.49

(20) Schmittel, M.; Ganz, A. *Chem. Commun.* **1997**, 999–1000.

(21) Kubas, G. J. *Inorg. Synth.* **1979**, 19, 90–91.

(22) Dietrich-Buchecker, C. O.; Marnot, P. A.; Sauvage, J.-P. *Tetrahedron Lett.* **1982**, 23, 5291–5294.

(23) Yamada, M.; Nakamura, Y.; Kuroda, S.; Shimao, I. *Bull. Chem. Soc. Jpn.* **1990**, 63, 2710–2712.

(24) Toyota, S.; Woods, C. R.; Benaglia, M.; Siegel, J. S. *Tetrahedron Lett.* **1998**, 39, 2697–2700.

(25) Sjörgen, M.; Hansson, S.; Norrby, P.-O.; Akermark, B.; Cucciolito, M. E.; Vitagliano, A. *Organometallics* **1992**, 11, 3954–3964.

Table 1. Crystallographic Data

compd	[Cu(dop) ₂](PF ₆)(C ₂ H ₅) ₂ O	[Cu(xop) ₂](PF ₆)- ³ / ₂ CH ₃ OH	[Cu(dpep) ₂](PF ₆)	[Cu(dmesp)(dpep)](PF ₆)
formula	CuC ₅₆ H ₅₀ F ₆ N ₄ OP	CuC ₅₅ H ₄₈ F ₆ N ₄ OP	CuC ₅₆ H ₃₂ F ₆ N ₄ P	CuC ₅₈ H ₄₄ F ₆ N ₄ P
color, habit	red blocks	red prisms	red plates	red prisms
cryst size (mm)	1.00 × 1.00 × 0.70	1.50 × 0.40 × 0.40	1.30 × 0.80 × 0.15	0.90 × 0.40 × 0.25
cryst syst	triclinic	monoclinic	triclinic	orthorhombic
space group	<i>P</i> 1	<i>C</i> 2/ <i>c</i>	<i>P</i> 1	<i>Pbca</i>
<i>a</i> (Å)	11.854(3)	23.096(6)	13.327(7)	14.547(6)
<i>b</i> (Å)	14.705(3)	23.387(6)	14.114(7)	22.868(6)
<i>c</i> (Å)	15.866(4)	17.873(7)	15.175(5)	30.659(10)
α (deg)	107.81(2)		87.23(4)	
β (deg)	106.72(2)	100.08(3)	66.48(3)	
γ (deg)	97.56(2)		61.84(4)	
<i>V</i> (Å ³)	2447.6(10)	9505(5)	2273(2)	10199(6)
<i>Z</i>	2	8	2	8
form wt	1003.51	989.5	969.37	1005.48
temp (K)	187	295	295	295
2θ range	3.32–45.00	3.18–50.00	3.32–45.00	3.56–40.00
reflns collected	8329	8664	6262	4749
indep reflns	8329	8382	5952	4749
reflns (<i>F</i> > 4σ(<i>F</i>))	5739	5631	4851	2281
<i>R</i> indices (obs data)	<i>R</i> = 7.52%; <i>R</i> _w = 19.09%	<i>R</i> = 6.02%; <i>R</i> _w = 14.53%	<i>R</i> = 5.47%; <i>R</i> _w = 14.45%	<i>R</i> = 9.43%; <i>R</i> _w = 20.44%
<i>R</i> indices (all data)	<i>R</i> = 11.49%; <i>R</i> _w = 23.48%	<i>R</i> = 9.46%; <i>R</i> _w = 17.53%	<i>R</i> = 6.78%; <i>R</i> _w = 15.99%	<i>R</i> = 19.10%; <i>R</i> _w = 27.45%
GOF	1.016	1.065	1.021	1.026
data-to-param ratio	13.5:1	13.4:1	9.7:1	14.2:1

(s, 6H), 1.74 (s, 12H), 5.94 (s, 4H), 6.30 (d, 4H), 7.01 (t, 4H), 7.27 (t, 2H), 8.02 (d, 2H), 8.08 (d, 2H), 8.14 (s, 2H), 8.31 (d, 2H), 8.73 (d, 2H), 8.88 (d, 2H).

Luminescence Measurements. Steady-state luminescence spectra were recorded on a Perkin-Elmer LS 50B luminescence spectrometer equipped with a red-sensitive photomultiplier tube. Spectra were corrected using the files supplied by the manufacturer which consisted of the average detector response of 10 instruments. Quantum yields of emission were determined in freeze–pump–thaw degassed dichloromethane using the optically dilute technique.²⁶ The quantum yield of the complex [Ru(bpy)₃](PF₆)₂ in nitrogen-purged water was used as a standard ($\Phi_{em} = 0.042$).²⁷ The refractive indices of water and dichloromethane were taken as 1.333 and 1.424, respectively.²⁸ The errors in Φ_{em} are estimated to be ±25%.

Time-resolved luminescence was studied using a pulsed dye laser at 445 nm, pumped by an XeCl excimer laser. About 2 mJ was available in a 4-ns pulse. Scattered excitation light was rejected by a glass cutoff filter. The emission wavelength was selected by a 0.25-m monochromator with an 8-nm band-pass and detected using an Amperex TUV56 photomultiplier, which is specially designed to give a linear response for large, pulsed anode currents. The photocurrent was digitized by a Lecroy 9361 oscilloscope. Several hundred signals could be averaged, but that was seldom necessary. Accumulated data files were transferred to a microcomputer and fit to a single exponential using a nonlinear least-squares algorithm, based on the Marquardt method.

Electrochemical Measurements. Cyclic voltammograms were recorded on a Bioanalytical Systems CV50W voltametric analyzer. Analysis was performed in a single compartment cell with a glassy carbon working electrode, a Pt wire counter electrode, and an Ag/AgCl(aq) reference electrode. The electrolyte, tetrabutylammonium hexafluorophosphate (TBAH), was recrystallized twice from a 50/50 (by volume) mixture of water and 95% ethanol. The electrolyte was then recrystallized from dichloromethane/diethyl ether, dried under vacuum, and stored in a glovebox. Immediately following analysis, ferrocene was added to the sample and the ferrocenium/ferrocene (Fc⁺/Fc) couple was recorded. The Fc⁺/Fc couple was also recorded versus a saturated calomel electrode (SCE) under identical solvent and electrolyte conditions. The Fc⁺/Fc couple was measured at 450 and 443 mV vs Ag/AgCl(aq) in dichloromethane and acetonitrile, respectively. The Fc⁺/Fc couple was measured at 450 and 404 mV vs SCE in dichloromethane and acetonitrile, respectively. The difference in

the Fc⁺/Fc couples was used to correct the measured potentials (vs Ag/AgCl(aq)) to an SCE reference electrode.

Crystal Structure Determinations. Data collection using Mo Kα radiation for the structure determinations of [Cu(dop)₂](PF₆), [Cu(xop)₂](PF₆), [Cu(dpep)₂](PF₆), and [Cu(dmesp)(dpep)](PF₆) utilized a Siemens R3m/V four-circle diffractometer. Data collection and crystal parameters are reported in Table 1. Each of the structures was solved by direct methods (SHELXTL PLUS). All non-hydrogen atoms were defined anisotropically, while the hydrogens were calculated and fixed in idealized positions (*d*(C–H) = 0.96 Å). Tables of positional parameters, bond lengths, bond angles, anisotropic thermal parameters, and ORTEP views of the complex cations are available in the Supporting Information.

Results and Discussion

The following five copper(I) complexes are of principal interest in this paper: [Cu(dpp)₂](PF₆), [Cu(dop)₂](PF₆), [Cu(xop)₂](PF₆), [Cu(dpep)₂](PF₆), and [Cu(dmesp)(dpep)](PF₆) (Chart 1). The complex [Cu(dpp)₂]⁺ serves as the reference compound for the majority of discussion since the crystal structure, electrochemistry, absorption spectroscopy, and photo-physic of the complex cation have been investigated previously by others.^{6,10–12} We recently reported the solid-state structure of [Cu(dpp)₂](PF₆), as well as an investigation of solution-state absorption spectra of the complex.⁸ Masood and Zacharias have previously investigated the electrochemistry²⁹ and emission spectra³⁰ of [Cu(dop)₂](BF₄) (these authors refer to the cation as [Cu(dtphen)₂]⁺). No structural data or excited-state lifetime data for [Cu(dop)₂]⁺ have, however, been previously reported.

(I) Preparation of the Copper Complexes. The homoleptic copper(I) complexes [Cu(dop)₂]⁺, [Cu(xop)₂]⁺, and [Cu(dpep)₂]⁺ were synthesized by the addition of a solution of 2 equiv of the ligand to one equivalent of tetra(acetonitrilo)-copper(I) hexafluorophosphate. The heteroleptic complex [Cu(dmesp)(dpep)]⁺ was synthesized by exploiting the fact that the dmesp ligand is too sterically demanding to form a 2:1 homoleptic complex with copper.²⁰ Thus, by adding 1 equiv of the sterically less demanding ligand dpep and 1 equiv of dmesp

(26) Demas, J. N.; Crosby, G. A. *J. Phys. Chem.* **1971**, *75*, 991–1024.

(27) Van Houten, J.; Watts, R. J. *J. Am. Chem. Soc.* **1976**, *98*, 4853–4858.

(28) *CRC Handbook of Chemistry and Physics*, 74th ed.; Lide, D. R., Ed.; CRC Press: Boca Raton, FL, 1993.

(29) Masood, M. A.; Zacharias, P. S. *J. Chem. Soc., Dalton Trans.* **1991**, 111–114.

(30) Masood, M. A.; Zacharias, P. S. *Trans. Met. Chem.* **1992**, *17*, 563–567.

to 1 equiv of copper(I), clean formation of $[\text{Cu}(\text{dmesp})(\text{dpep})]^+$ results. Schmittel and Ganz have shown that this is a general phenomenon for copper(I) bis(phenanthroline) complexes that appears to result from the fact that at room temperature these complexes are in a rapid dissociation–association equilibrium.²⁰ Thus, stoichiometric control of the ligands available to copper(I) results in exclusive formation of heteroleptic complexes such as $[\text{Cu}(\text{dmesp})(\text{dpep})]^+$, since this is the only possible situation that results in all of the copper ions coordinated to four phenanthroline nitrogens (i.e., in a $[\text{Cu}(\text{NN})_2]^+$ coordination sphere).

(II) Electronic Absorption Spectra. The absorption spectra of the copper(I) complexes in dichloromethane are shown in Figure 1. All of the complexes absorb over a broad region of the visible spectrum. These bands result from several MLCT transitions that have been previously assigned.^{31,32} Comparing the visible spectra of the four complexes $[\text{Cu}(\text{dop})_2]^+$, $[\text{Cu}(\text{xop})_2]^+$, $[\text{Cu}(\text{dpep})_2]^+$, and $[\text{Cu}(\text{dmesp})(\text{dpep})]^+$ to that of $[\text{Cu}(\text{dpp})_2]^+$, there are notable differences. For $[\text{Cu}(\text{dpp})_2]^+$, the low-energy shoulder in the 550–600 nm range has been attributed to result from a molecular distortion of the complex from D_{2d} symmetry.^{10,33} This low-symmetry conformation likely occurs to maximize intramolecular π -stacking interactions between opposing ligands. These interactions are clearly seen in the solid-state structure (vide infra). Thus, the intensity of the low-energy shoulder is a rough measure of the distortion away from D_{2d} symmetry. Conversely, as the more sterically demanding ligands impart more rigidity to the complex and enforce D_{2d} symmetry, the low-energy shoulder should decrease. On the basis of the intensities of the low-energy MLCT bands in Figure 1, the complexes are ranked in terms of increasing rigidity as follows: $[\text{Cu}(\text{dpep})_2]^+ \leq [\text{Cu}(\text{dpp})_2]^+ < [\text{Cu}(\text{dmesp})(\text{dpep})]^+ < [\text{Cu}(\text{dop})_2]^+ < [\text{Cu}(\text{xop})_2]^+$. This trend is consistent with what one would predict for the rigidity of the copper coordination sphere on the basis of the molecular models. In addition to the variation in the intensity of the low-energy shoulders, the position of the MLCT absorption maxima vary over the series of complexes from 440 to 500 nm. However, no trend consistent with an electronic or steric effect is evident to explain these shifts.

Analysis of the charge-transfer absorption intensities (i.e., oscillator strengths) should provide an indication of the amount of ligand electronic delocalization in the complexes.^{16,19,34,35} An experimental measure of the oscillator strength of a complex can be obtained from the absorption spectrum since the oscillator strength is proportional to the integrated area under the absorption manifold.³⁴ The relative absorption intensities for the five copper(I) complexes were determined by integrating the absorption spectra of the complexes from 14 286 to 25 000 cm^{-1} , and are as follows (arbitrary units): $[\text{Cu}(\text{xop})_2]^+$, 141; $[\text{Cu}(\text{dop})_2]^+$, 226; $[\text{Cu}(\text{dpp})_2]^+$, 233; $[\text{Cu}(\text{dmesp})(\text{dpep})]^+$, 280; $[\text{Cu}(\text{dpep})_2]^+$, 306. The trend in these values does agree with the amount of ligand π -delocalization that is predicted a priori (see Introduction). However, compared to other MLCT systems where ligand delocalization is varied,^{16,19,35} the absorption differences among the five complexes are quite small.

The absorption spectra of the five complexes were also investigated in acetonitrile. Relative to the spectra in dichloro-

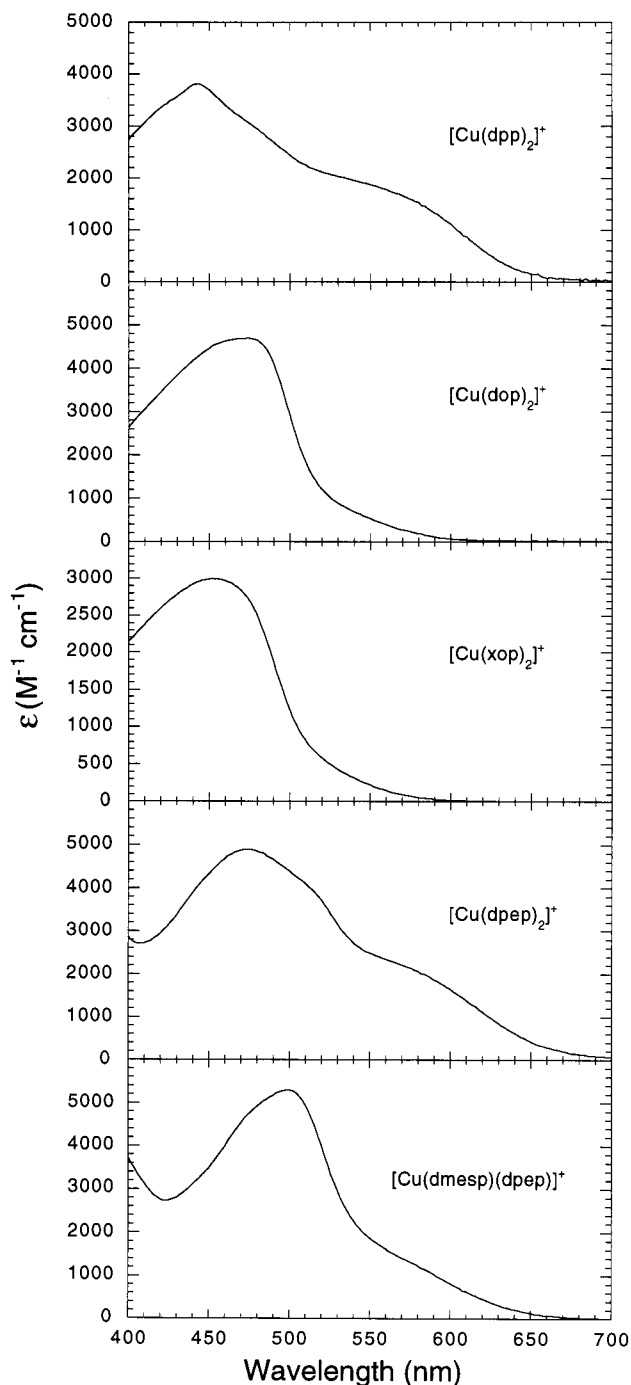


Figure 1. Electronic absorption spectra of the copper(I) complexes in dichloromethane at room temperature.

methane, the spectra in acetonitrile are essentially the same, with one exception. The $[\text{Cu}(\text{xop})_2]^+$ complex dissociates to a large degree in acetonitrile to the mono-phenanthroline complex $[\text{Cu}(\text{xop})]^+$. This dissociation is evidenced by the appearance of a new shoulder at 360 nm which is assigned to $[\text{Cu}(\text{xop})]^+$ (see Supporting Information). Very similar behavior was observed by Eggleston et al. with the copper(I) complex of 2,9-di-*neo*-pentyl-1,10-phenanthroline, $[\text{Cu}(\text{dnpp})_2]^+$.⁹ The $[\text{Cu}(\text{dnpp})_2]^+$ complex is stable in dichloromethane and dissociates somewhat in acetonitrile. All of these results are useful in demonstrating that the complexes $[\text{Cu}(\text{xop})_2]^+$ and $[\text{Cu}(\text{dnpp})_2]^+$ appear to be at, or near, the steric limit that allows for formation of the bis(phenanthroline) complex in a non-coordinating solvent.

(31) Parker, W. L.; Crosby, G. A. *J. Phys. Chem.* **1989**, *93*, 5692–5696.

(32) Everly, R. M.; McMillin, D. R. *J. Phys. Chem.* **1991**, *95*, 9071–9075.

(33) Klemens, F. K.; Palmer, C. E. A.; Rolland, S. M.; Fanwick, P. E.; McMillin, D. R.; Sauvage, J.-P. *New J. Chem.* **1990**, *14*, 129–133.

(34) Phifer, C. C.; McMillin, D. R. *Inorg. Chem.* **1986**, *25*, 1329–1333.

(35) Hecker, C. R.; Gushurst, A. K. I.; McMillin, D. R. *Inorg. Chem.* **1991**, *30*, 538–541.

Table 2. Electrochemical Data

compound	CH ₂ Cl ₂ ^a		CH ₃ CN ^a	
	Cu(L) ₂ ^{2+/+} (ΔE _p)	Cu(L) ₂ ^{2+/+} (ΔE _p)	Cu(L) ₂ ⁺⁰ (ΔE _p)	Cu(L) ₂ ^{0/-1} (ΔE _p)
[Cu(dpp) ₂](PF ₆)	0.84 (70)	0.70 (59)	-1.66 (60)	<i>i</i>
[Cu(dop) ₂](PF ₆)	1.00 (62)	0.87 (69)	-1.69 (69)	-1.96 (60)
[Cu(xop) ₂](PF ₆)	1.03 (64)	0.90 (100)	-1.56 (74)	<i>i</i>
[Cu(dmesp)(dpep)]-(PF ₆)	0.92 (60)	0.84 (86)	-1.47 (59)	<i>i</i>
[Cu(dpep) ₂](PF ₆)	0.87 (72)	0.69 (116)	-1.36 (59)	<i>i</i>

^a Redox couples were measured in a nitrogen saturated solution containing 0.1 M TBAH at room temperature. Couples are reported in volts vs SCE. *i* = irreversible. The difference between the anodic and cathodic current peak potential (in mV) is given in parentheses.

(III) Electrochemical Properties. The cyclic voltammograms of the complexes were recorded in dichloromethane and in acetonitrile (Table 2). Previous studies have shown that the potential of the Cu^{2+/+} couple in [Cu(NN)₂]⁺ systems with 2 and 9 phenanthroline substituents is influenced to a large degree by the sterics of the substituents.^{9,36} In general, as the steric bulk of the 2 and 9 substituents increases, the ligands are less able to rearrange to the preferred (square-planar) coordination geometry of Cu²⁺ due to steric clashes with the opposing ligand. This stabilizes the Cu⁺ state and results in an increase in the Cu^{2+/+} redox potential. Thus, assuming there are no extreme changes in the electron-donating or -withdrawing properties of the ligands, this redox couple can be used to indicate the rigidity the ligands impart on the complex by observing the shift in the Cu^{2+/+} redox potentials. Based on the electrochemical studies in dichloromethane (the solvent in which the oxidative couples are more accurately determined) (Table 2), the complexes are ranked in terms of increasing rigidity as follows: [Cu(dpp)₂]⁺ < [Cu(dpep)₂]⁺ < [Cu(dmesp)(dpep)]⁺ < [Cu(dop)₂]⁺ < [Cu(xop)₂]⁺. This trend is similar to the trend in rigidity obtained from analysis of the absorption spectra in dichloromethane (vide supra).

Upon reduction in acetonitrile, all of the complexes display a reversible couple corresponding to a single ligand reduction and formation of [Cu(L)(L⁻)]⁰. Reversible formation of the singly reduced species has been previously observed with several [Cu(NN)₂]⁺ complexes.^{9,29} Interestingly, the [Cu(dop)₂]⁺ complex also displays reversible formation of the doubly reduced species in acetonitrile (Table 2). Reversible formation of the doubly reduced species has been observed for the copper(I) catenates,³⁶ however, has not been previously observed with a simple [Cu(NN)₂]⁺ complex.

(IV) Solution-State Structural Properties. The ¹H NMR spectra of the complexes were examined in order to ascertain whether rigidifying the copper coordination environment would affect averaging processes on the NMR time scale. In DMSO-*d*₆, well-resolved signals were observed for all of the protons in each of the five complexes (see Experimental Section). It is likely that in dms, all of the complexes are in a rapid dissociation-association equilibrium. However in CDCl₃, significant differences were observed for the complexes [Cu(dpp)₂]⁺, [Cu(dop)₂]⁺, and [Cu(xop)₂]⁺. Whereas the aromatic proton signals are significantly broadened in [Cu(dpp)₂]⁺ at room temperature, some of the aromatic signals sharpen somewhat in [Cu(dop)₂]⁺, and all of the signals become very sharp and completely resolved in [Cu(xop)₂]⁺ (see Supporting Information). Previous work has shown that in a catenane with

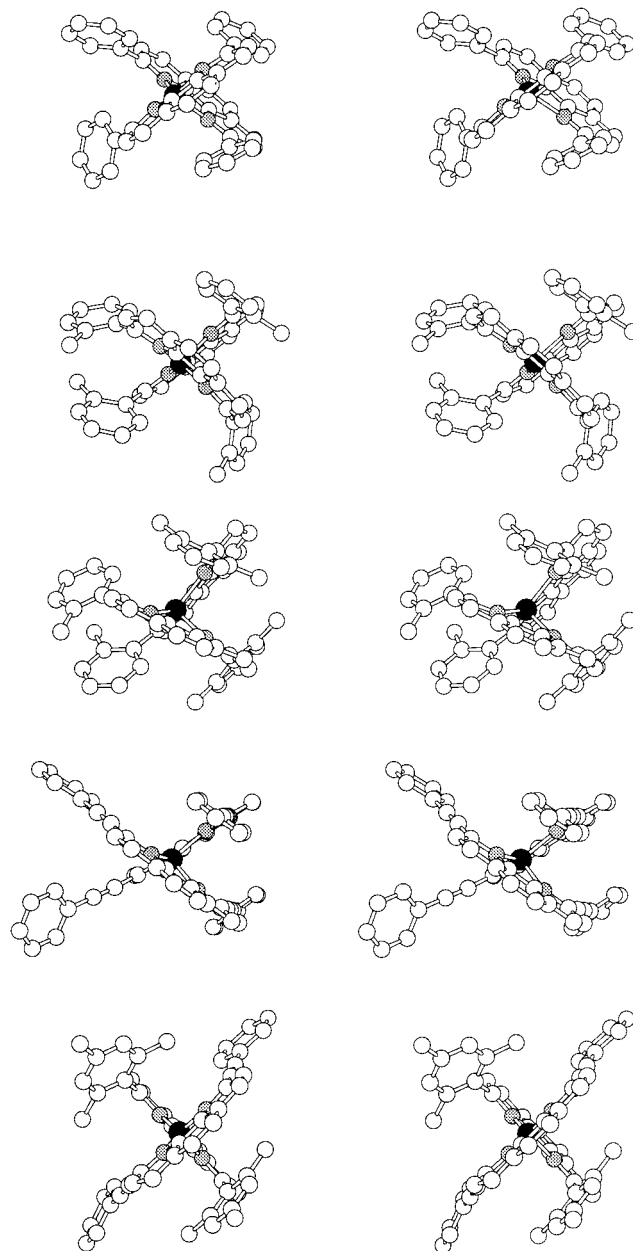


Figure 2. Stereoviews of the copper(I) complexes. From top to bottom: [Cu(dpp)₂]⁺, [Cu(dop)₂]⁺, [Cu(xop)₂]⁺, [Cu(dpep)₂]⁺, [Cu(dmesp)(dpep)]⁺.

a [Cu(dpp)₂]⁺ moiety (Cu(cat-30)⁺), the phenyl substituents are free to rotate relative to the phenanthroline group on the NMR time scale.¹¹ It can be concluded from these results that at room temperature in CDCl₃, the rotational freedom of the aryl substituents in the ligands dop and xop is significantly reduced. And in the case of [Cu(xop)₂]⁺, this lack of rotational freedom combined with interligand interactions force the coordination environment to be highly rigid at room temperature.

(V) Solid-State Structural Properties. Each of the five copper(I) complexes under investigation have been crystallographically characterized. The structure of [Cu(dpp)₂]⁺ was first reported with (CuCl₂)⁻ as the anion,³³ and more recently as the (PF₆)⁻ complex.⁸ Here we report the structures of [Cu(dop)₂](PF₆), [Cu(xop)₂](PF₆), [Cu(dpep)₂](PF₆), and [Cu(dmesp)(dpep)](PF₆) (Table 1). In Figure 2 are shown the stereoviews of the four new copper(I) complexes and the [Cu(dpp)₂]⁺ complex for comparison. As described before for [Cu(dpp)₂]⁺,^{8,33} and as seen in Figure 2 for the four new

(36) Federlin, P.; Kern, J.-M.; Rastegar, A.; Dietrich-Buchecker, C.; Marnot, P. A.; Sauvage, J.-P. *Nouv. J. Chim.* **1990**, *14*, 9–12.

Table 3. Selected Structural Data

	[Cu(dop) ₂](PF ₆)	[Cu(xop) ₂](PF ₆)	[Cu(dpep) ₂](PF ₆)	[Cu(dmesp)(dpep)](PF ₆)
Cu–N1A (Å)	2.133(5)	2.002(3)	2.087(3)	2.041(6)
Cu–N2A (Å)	2.006(5)	2.136(3)	2.000(3)	1.985(6)
Cu–N1B (Å)	2.077(4)	2.018(3)	2.081(3)	2.041(5)
Cu–N2B (Å)	2.025(5)	2.131(3)	2.003(3)	1.989(6)
N1A–Cu–N2A (deg)	81.5(2)	81.26(13)	81.61(13)	83.1(2)
N2B–Cu–N1A (deg)	117.3(2)	120.74(13)	126.14(13)	126.6(2)
N1B–Cu–N1A (deg)	107.6(2)	143.59(13)	101.22(13)	115.0(2)
N2B–Cu–N2A (deg)	136.4(2)	104.77(12)	139.00(13)	133.9(2)
N1B–Cu–N2A (deg)	132.2(2)	122.99(12)	126.61(13)	118.5(2)
N1B–Cu–N2B (deg)	82.02(2)	81.86(12)	81.30(14)	83.0(2)
θ _x (deg)	71.6	75.4	76.5	78.6
θ _y (deg)	84.0	72.9	73.4	85.6
θ _z (deg)	84.8	85.7	77.9	89.5
Phenanthroline–Aryl Dihedral Angles ^a				
A–C (deg)	64.0	56.3	69.4	14.1
A–D (deg)	55.9	80.1	49.2	25.0
B–E (deg)	60.5	49.7	66.5	81.3
B–F (deg)	51.7	81.8	7.0	88.7

^a The phenanthroline planes are labeled A and B in each complex, and the aryl substituents are labeled C through F. In [Cu(xop)₂](PF₆), the xylyl planes are D and F; in [Cu(dmesp)(dpep)](PF₆), the mesityl planes are E and F.

structures, a prominent feature of these structures is intramolecular interligand π -stacking interactions. Two aryl-phenanthroline stacking interactions are observed for each of [Cu(dpp)₂]⁺, [Cu(xop)₂]⁺, and [Cu(dpep)₂]⁺. One aryl-phenanthroline stacking interaction is observed in each of [Cu(dop)₂]⁺ and [Cu(dmesp)(dpep)]⁺ (Figure 2). Notably, the structure of [Cu(dpep)₂]⁺ is remarkably similar to the structure of [Cu(dpp)₂]⁺, consistent with the similar visible spectral features observed for these two complexes in Figure 1.

Clearly, π -delocalization involving the aryl groups is dependent upon the dihedral angles between the phenanthroline and aryl groups. The structures of [Cu(dop)₂]⁺ and [Cu(xop)₂]⁺ demonstrate that the ortho methyl groups have a notable effect on the orientation of the 2- and 9-aryl substituents relative to the phenanthroline moiety. In the structure of [Cu(dpp)₂](PF₆), the average dihedral angle between the phenyl substituents and the phenanthroline planes is 52°. In [Cu(dop)₂]⁺ and [Cu(xop)₂]⁺, the average dihedral angles are 58° and 67°, respectively (Table 3). The xylyl substituents in [Cu(xop)₂]⁺ are very close to an orthogonal conformation relative to the phenanthroline planes with dihedral angles of 80.1° and 81.8° (Figure 2, Table 3). Similar conformations are also observed for the mesityl substituents in the structure of [Cu(dmesp)(dpep)]⁺ (dihedral angles of 81.3° and 88.7°).

The primary impetus for investigation of the solid-state structures of these complexes was to determine the effects that the 2 and 9 substituents have on the copper coordination environment (Table 3). As seen in Figure 2, all of the complexes display distorted tetrahedral environments about the copper ions. The distortion from D_{2d} symmetry can be described in terms of the angles θ_x , θ_y , and θ_z (for D_{2d} , $\theta_x = \theta_y = \theta_z = 90^\circ$).³⁷ The average θ value (θ_{av}) for [Cu(dpp)₂]⁺ in the PF₆⁻ and CuCl₂⁻ complexes is 75.0° and 73.8°, respectively.^{8,33} Our present results demonstrate that θ_{av} is approximately the same for [Cu(dpep)₂]⁺ (75.9°), goes up for [Cu(dop)₂]⁺ and [Cu(xop)₂]⁺ (80.1° and 78.0°), and is the largest for [Cu(dmesp)(dpep)]⁺ (84.6°). These results are in good agreement with the analysis of the copper coordination environments provided by the absorption spectra (vide supra), except for the [Cu(dmesp)(dpep)]⁺ complex. On the basis of the intensity

of the low-energy MLCT shoulder, [Cu(dmesp)(dpep)]⁺ was assigned a geometry intermediate between [Cu(dop)₂]⁺ and [Cu(dpp)₂]⁺. The θ_{av} value, however, places this complex as the closest to D_{2d} symmetry. This apparent anomaly between the absorption data and the solid-state data is conceivably explained by the reduction of molecular symmetry in [Cu(dmesp)(dpep)]⁺. Thus, the intensity of the low-energy MLCT band in the heteroleptic complex is perhaps not a direct measure of the distortion of the copper coordination environment since it could in part result from the asymmetric ligand environment.

Nonetheless, within the limitations inherent in solid-state vs solution-state comparisons, the crystal structures generally agree with the structures of the complexes in solution as revealed by electronic absorption and NMR spectroscopies.

(VI) Photophysical Properties. The room-temperature excited-state lifetimes, emission spectra, and quantum yields of the five copper(I) complexes were investigated in dichloromethane (Table 4). In addition, the excited-state lifetimes of [Cu(dpp)₂]⁺, [Cu(dop)₂]⁺, and [Cu(xop)₂]⁺ were investigated in methanol. A primary goal of this study was to identify the trend in the photophysical properties for the three complexes [Cu(dpp)₂]⁺, [Cu(dop)₂]⁺, and [Cu(xop)₂]⁺. The results in Table 4 show that the emission maxima are blue-shifted by 17 nm for the dop and xop complexes relative to the dpp complex. As outlined above, upon increasing the interligand steric interactions in the series [Cu(dpp)₂]⁺ < [Cu(dop)₂]⁺ < [Cu(xop)₂]⁺, the solid-state, spectral, and electrochemical results all predict that the flattening distortion will be reduced, and the energy gap will be larger for the latter two complexes. This is consistent with the blue-shifted emission spectra for the dop and xop complexes.

As seen in Table 4, the excited-state lifetimes in dichloromethane decrease in the series [Cu(dpp)₂]⁺ > [Cu(dop)₂]⁺ > [Cu(xop)₂]⁺ as follows: 243 ns, 182 ns, 149 ns. In the study of the photophysical properties of transition-metal complexes, it is often instructive to break down the observed decay rate constant ($k_{obs} = 1/\tau$) into the radiative decay rate constant ($k_r = \phi/\tau$) and the nonradiative decay rate constant ($k_{nr} = (1 - \phi)/\tau$).¹³ Such a breakdown is somewhat complicated in the study of copper(I) bis(phenanthroline) complexes. In analyzing the emission spectra of a series of [Cu(NN)₂]⁺ complexes at various temperatures, Kirchoff et al. showed that these

(37) Dobson, J. F.; Green, B. E.; Healy, P. C.; Kennard, C. H. L.; Pakawatchai, C.; White, A. H. *Aust. J. Chem.* **1984**, *37*, 649–659.

Table 4. Room-Temperature Photophysical Data

compound	CH ₂ Cl ₂						CH ₃ OH
	$\lambda_{\text{max}}^{\text{abs}}, \text{nm}^a$	$\lambda_{\text{max}}^{\text{em}}, \text{nm}^b$	$\Phi_{\text{em}} \times 10^{-4}^c$	τ, ns^d	$k_{\text{r}}^{\text{eff}}, \text{s}^{-1} \times 10^3^e$	$k_{\text{nr}}^{\text{eff}}, \text{s}^{-1} \times 10^6^e$	τ, ns^f
[Cu(dpp) ₂](PF ₆)	440 (3800)	690	8.7	243	3.6	4.1	131
[Cu(dop) ₂](PF ₆)	472 (4700)	673	15	182	8.2	5.5	107
[Cu(xop) ₂](PF ₆)	452 (3.0 × 10 ³)	673	10	149	6.7	6.7	81
[Cu(dmesp)(dpep)](PF ₆)	500 (5300)			<20			
[Cu(dpep) ₂](PF ₆)	474 (4900)						

^a The molar extinction coefficient at the absorption maximum (M⁻¹ cm⁻¹) is given in parentheses. ^b From corrected photoluminescence spectra (± 5 nm) (see text for details) with excitation at 450 nm. ^c Photoluminescence quantum yields were determined in deoxygenated dichloromethane (see text for details) with excitation at 450 nm. ^d Excited-state lifetime in deoxygenated dichloromethane ($\pm 5\%$) with excitation at 445 nm. ^e Effective radiative and nonradiative rate constants (see text for details). ^f Excited-state lifetime in deoxygenated methanol ($\pm 5\%$) with excitation at 445 nm.

complexes actually emit from two excited states (assigned as a singlet and a triplet) that are in thermal equilibrium.³⁸ Without performing analogous studies, we assume that all of the complexes under investigation in this report are similar in that the emission actually occurs from two thermally equilibrated excited states. Thus, true k_{r} and k_{nr} values cannot simply be calculated. However, since all of the luminescent decay traces we observe are single exponential, we can treat the photophysical properties of these complexes as arising from a single excited state having the averaged properties of the two contributors (as is usually done for tris(diimine) complexes of ruthenium(II) that also emit from more than one MLCT excited state at room temperature¹³). The effective rate constants ($k_{\text{r}}^{\text{eff}}$ and $k_{\text{nr}}^{\text{eff}}$ at 25 °C) are found in Table 4. One trend that we observe is that the $k_{\text{r}}^{\text{eff}}$ values are greater for both the dop and xop complexes relative to the dpp complex. Since the value of the radiative rate constant is proportional to the cube of the radiative energy gap,^{16,19} these results are understandable from the blue-shifted emission maxima for these complexes. The difference observed in the $k_{\text{r}}^{\text{eff}}$ values *between* the xop and dop complexes (Table 4) is however reasonably small when one considers the fairly large errors associated with the determination of the quantum yields (see Experimental Section).

In analyzing the $k_{\text{nr}}^{\text{eff}}$ values, the trend we observe is almost a monotonic increase from [Cu(dpp)₂]⁺ to [Cu(dop)₂]⁺ to [Cu(xop)₂]⁺ (Table 4). In the complexes under investigation, the quantum yields are sufficiently small that the $k_{\text{nr}}^{\text{eff}}$ values are essentially the same as k_{obs} and are thus simply calculated as $1/\tau$. Since the errors associated with the lifetime determinations are at most $\pm 5\%$, the trends observed in the $k_{\text{nr}}^{\text{eff}}$ values are very reliable. In view of the fact that the dop and xop complexes emit at higher energy relative to the dpp complex, one prediction based on the energy-gap law would be that the $k_{\text{nr}}^{\text{eff}}$ values should be smaller for the dop and xop complexes (i.e., the dop and xop complexes should display longer excited-state lifetimes).¹³ This prediction is based on the assumption that there will be decreased vibrational overlap between the ground and excited states when the energy gap is larger. In fact, this is precisely what Eggleston et al. observed in their study where the steric bulk of the 2- and 9-alkyl substituents was varied systematically in a series of [Cu(NN)₂]⁺ complexes.⁹ Upon increasing the steric requirements of the alkyl substituents, Eggleston et al. found that the emission maxima were blue-shifted and the $k_{\text{nr}}^{\text{eff}}$ values decreased.

The major difference between our study of [Cu(dpp)₂]⁺, [Cu(dop)₂]⁺, and [Cu(xop)₂]⁺ and Eggleston et al.'s study, is that the 2 and 9 substituents in the present study are not electronically similar in their ability to affect ligand π -delocal-

ization. The focus of this work was to determine if the phenyl substituents in [Cu(dpp)₂]⁺ were affecting the photophysical properties of the complex simply via the steric properties of the substituent, or also via π -delocalization. As described above, the solution NMR data indicate that the aryl groups in [Cu(dop)₂]⁺ and [Cu(xop)₂]⁺ are not rotating freely relative to the phenanthroline groups, thus reducing the ability for extended π -delocalization. We therefore interpret the photophysical results to indicate that reduction in the amount of π -delocalization in the dop and xop ligands in the excited-state is the primary cause for the larger $k_{\text{nr}}^{\text{eff}}$ values relative to the dpp complex. Although the energy gap in the dop and xop complexes is larger than in the dpp complex, the amount of π -delocalization is reduced in the former complexes. A larger energy gap and decreased delocalization should affect k_{nr} in opposite directions. Since the $k_{\text{nr}}^{\text{eff}}$ values are larger, we conclude delocalization plays the primary role. The result is that the dop and xop complexes emit at higher energy, and yet display shorter excited-state lifetimes than the dpp complex.

The variation in $k_{\text{nr}}^{\text{eff}}$ values over the series [Cu(dpp)₂]⁺, [Cu(dop)₂]⁺, and [Cu(xop)₂]⁺ could also simply be due to the additional methyl groups in the latter two complexes. The additional C–H vibrations could thus affect the nonradiative decay pathways in [Cu(dop)₂]⁺ and [Cu(xop)₂]⁺. We discount this as a significant contributing factor since Damrauer et al. have investigated the photophysical properties of a series of [Ru(2,2'-bipyridyl)₃]²⁺ complexes with phenyl and tolyl substituents on the bipyridyl ligands.¹⁹ The position of the methyl group on the tolyl substituent was varied, so as to decrease π -delocalization into the aryl group (via steric interactions), or not affect it at all. It was observed that if the additional methyl groups on the aryl substituents were not capable of affecting π -delocalization that the k_{nr} values were not significantly affected (compare [Ru(dptb)₃]²⁺ to [Ru(dpb)₃]²⁺). Yet, if π -delocalization into the aryl groups was decreased sterically, a larger effect on k_{nr} was observed (compare [Ru(dotb)₃]²⁺ to [Ru(dpb)₃]²⁺).

The excited-state lifetimes of [Cu(dpp)₂]⁺, [Cu(dop)₂]⁺, and [Cu(xop)₂]⁺ in methanol display a very similar trend to that observed in dichloromethane (Table 4). Relative to [Cu(dpp)₂]⁺, the k_{obs} values in methanol increase by 22% and 62% for [Cu(dop)₂]⁺ and [Cu(xop)₂]⁺, respectively. In dichloromethane, the k_{obs} values increase by 34% and 63% for the dop and xop complexes. Thus, the conclusions presented above regarding ligand π -delocalization appear to apply in the donating solvent methanol as well.

The photophysical properties of the two complexes [Cu(dpep)₂]⁺ and [Cu(dmesp)(dpep)]⁺ were also investigated in dichloromethane in order to observe the effects of increased ligand π -delocalization. The absorption spectra of these complexes (vide supra) demonstrate that ligand π -delocalization is

(38) Kirchhoff, J. R.; Gamache, R. E., Jr.; Blaskie, M. W.; Del Paggio, A. A.; Lengel, R. K.; McMillin, D. R. *Inorg. Chem.* **1983**, *22*, 2380–2384.

increased relative to $[\text{Cu}(\text{dpp})_2]^+$. We observe, however, that neither complex displays steady-state emission at room temperature in dichloromethane. A very short-lived decay ($\tau < 20$ ns) is observed at 650 nm for $[\text{Cu}(\text{dmesp})(\text{dpep})]^+$ upon pulsed laser excitation. Additionally, in the solid state, we observe no emission from either of the complexes $[\text{Cu}(\text{dpep})_2](\text{PF}_6)$ or $[\text{Cu}(\text{dmesp})(\text{dpep})](\text{PF}_6)$. A reasonable explanation for the lack of long-lived excited states in these complexes is that the acetylene group intramolecularly deactivates the excited state via a copper–acetylene interaction, akin to solvent-induced exciplex quenching. Although solution-state (dichloromethane) IR spectroscopy does not indicate any observable shift in the $\text{C}\equiv\text{C}$ stretch in the copper(I) complexes relative to the dpep ligand,³⁹ molecular models indicate that a slightly distorted excited state may permit this type of interaction. In fact, Ziessel, Suffert, and Youinou have stated that in a copper(I) complex structurally similar to $[\text{Cu}(\text{dpep})_2]^+$, solution and solid-state data indicate a “weak interaction between metal center and triple bonds.”⁴⁰ Their complex is based on 2,2'-bipyridyl ligands, which are slightly more flexible than phenanthrolines. Thus, the conformational flexibility of the bipyridyl ligands may allow an increased interaction between the ethynyl groups and the copper center in the ground state, whereas this interaction only occurs in the excited states of our complexes. An additional possibility that would explain the lack of emission in $[\text{Cu}(\text{dpep})_2]^+$ and $[\text{Cu}(\text{dmesp})(\text{dpep})]^+$ is that the phenylethynyl substituents are not sterically effective in preventing excited-state distortion.

Conclusions

The present investigation and the investigation by Eggleston et al.⁹ combine to show that there are at least two major structural distortions that occur in the MLCT excited states of $[\text{Cu}(\text{NN})_2]^+$ complexes that impact on their photophysical properties. To enhance the photophysical properties

of these complexes, a reduction of these excited-state distortions is an important objective. One distortion involves the relative orientation of the two phenanthroline ligands and is the “flattening” distortion. This occurs because of the preferences of the copper(II) ion for a square-planar coordination environment. Reduction of this distortion has been accomplished in an interligand fashion by Eggleston et al. by increasing the steric bulk of the 2 and 9 substituents.⁹ Substituents that are too large, however, prevent formation of the bis(phenanthroline) complexes, indicating that there is likely an optimum size for these substituents. The second major distortion in the MLCT excited-state involves a single ligand, since the excited electron will be delocalized over the π^* -system of one ligand as the radical anion. A reduction of this type of distortion can be achieved by utilizing substituents that increase the π -delocalization. Our results indicate that the phenyl substituents in $[\text{Cu}(\text{dpp})_2]^+$ reduce both types of structural distortion. It is also apparent that the specific positioning of the phenanthroline substituents is just as important in affecting the photophysical properties as the nature of the substituents themselves. In the case of $[\text{Cu}(\text{dpep})_2]^+$ and $[\text{Cu}(\text{dmesp})(\text{dpep})]^+$, intramolecular quenching by a substituent phenylethynyl group may be operative. Careful consideration of these issues is necessary in order to optimize the photophysical properties of $[\text{Cu}(\text{NN})_2]^+$ complexes.

Acknowledgment. Partial support for this work was provided through a Hellman Faculty Fellowship (to T.B.K.). We thank Professor D. Magde for the use of his pulsed laser equipment, Professor Y. Tor for the use of his emission spectrometer, Professor W. Trogler for the use of his IR spectrometer, Craig Woods for the sample of dmesp, and Professor J. Siegel for helpful discussions.

Supporting Information Available: Tables of positional parameters, bond lengths, bond angles, anisotropic thermal parameters, and ORTEP diagrams for the four crystal structures; UV-spectra of $[\text{Cu}(\text{dpp})_2]^+$, $[\text{Cu}(\text{dop})_2]^+$, and $[\text{Cu}(\text{xop})_2]^+$ in acetonitrile; NMR spectra of $[\text{Cu}(\text{dpp})_2]^+$, $[\text{Cu}(\text{dop})_2]^+$, and $[\text{Cu}(\text{xop})_2]^+$ in CDCl_3 ; and an X-ray crystallographic file, in CIF format. This material is available free of charge via the Internet at <http://pubs.acs.org>.

IC9900399

(39) Munakata, M.; Kitagawa, S.; Kawada, I.; Maekawa, M.; Shimono, H. *J. Chem. Soc., Dalton Trans.* **1992**, 2225–2230.

(40) Ziessel, R.; Suffert, J.; Youinou, M.-T. *J. Org. Chem.* **1996**, *61*, 6535–6546.